

A time-of-flight application for nuclear reactions at Coulomb energies

M. G. PELLEGRITI⁽¹⁾(*), A. MUSUMARRA⁽¹⁾(²), E. DE FILIPPO⁽¹⁾,
M. DE NAPOLI⁽¹⁾, A. DI PIETRO⁽³⁾, P. FIGUERA⁽³⁾, M. FISICHELLA⁽³⁾,
I. LOMBARDO⁽¹⁾, C. MAIOLINO⁽³⁾, T. MARCHI⁽⁴⁾, D. RIFUGGIATO⁽³⁾,
D. SANTONOCITO⁽³⁾, V. SCUDERI⁽³⁾, E. STRANO⁽⁵⁾(⁶) and D. TORRESI⁽³⁾

⁽¹⁾ INFN, Sezione di Catania - Catania, Italy

⁽²⁾ Dipartimento di Fisica e Astronomia, Università di Catania - Catania, Italy

⁽³⁾ INFN, Laboratori Nazionali del Sud - Catania, Italy

⁽⁴⁾ INFN, Laboratori Nazionali di Legnaro - Legnaro, Italy

⁽⁵⁾ Dipartimento di Fisica, Università di Padova - Padova, Italy

⁽⁶⁾ INFN, Sezione di Padova - Padova, Italy

received 2 March 2020

Summary. — The Thick-Target Inverse Kinematics Resonant Scattering Method is an important tool for investigating resonances of the compound nucleus, spanning a wide center-of-mass energy range by using a single mono-energetic heavy-ion beam. The thick target can be solid (point-like) or gaseous. Anyhow, a limit of such a technique is related to the possible energy overlap of the same ejectile produced by different reaction mechanisms. These ejectiles have different paths inside the target allowing Time-of-Flight (ToF) discrimination. Thus, in order to disentangle different reaction channels and to get, for example, a clean elastic cross-section excitation function, a ToF event by event measurement can be performed in the case of gaseous targets. Several elastic scattering measurements on ⁴He gas targets were performed by using light ions. In this paper, the preliminary results of a heavy ion beam ($A = 208$) impinging on a ⁴He gas target at energies around the Coulomb barrier will be shown.

1. – Introduction

The Thick Target Inverse Kinematics Resonant Scattering Method (TTIK) [1-3] is widely used in order to measure elastic cross-sections induced by light ions and to determine resonance parameters in the compound nucleus. The technique is perfectly suited

(*) E-mail: mariagrazia.pellegriti@ct.infn.it

to the case of low intensity exotic beams, since it allows to explore a wide excitation energy range with a single beam energy, thus reducing the acquisition time. In this paper, the main characteristics of this method will be described and the criteria used in the choice of the target thickness will be indicated. In the case of gaseous targets, the ToF technique will be applied to disentangle elastic scattering contributions from inelastic ones. This last application will be described specifically for a heavy ion induced elastic scattering: ^{208}Pb on ^4He target.

2. – Thick target inverse kinematics resonant scattering method

The TTIK resonant elastic scattering method allows the study of a resonant state in the compound nucleus from the behaviour of the detected recoil yield. The beam energy loss in the target is used to continuously induce the elastic scattering in a given center-of-mass energy, E_{CM} , range. Since the projectile is heavier than the target nucleus, in inverse kinematics, light recoils (typically protons or alpha particles) are forward focused and with negligible energy loss in the target. Interference effects, due to the presence of both nuclear and Coulomb contribution, shows up in the recoil yield spectrum. The cross-section is equal to the square modulus of the scattering wave amplitude which is given by the equation

$$(1) \quad f = f_N + \delta f_C,$$

where f_N and f_C are the nuclear and the Coulomb scattering amplitudes respectively and δ is the Kronecker function, equal to one for elastic scattering and equal to zero for inelastic scattering.

When E_{CM} is approaching a resonance state in the compound nucleus, it is possible to observe an interference pattern in the case of elastic scattering and a Breit-Wigner shape in the case of the inelastic scattering. An R-matrix fit of the experimental cross-section allows to obtain precise information on resonance energies, orbital momenta and particle widths [3, 4].

3. – Choice of target thickness

The choice of a proper target thickness is essential for implementing this method. A general overview of the level scheme can be provided by using a thick target which stops completely the beam particles. To obtain more precise information on the investigated levels, with less straggling for the outgoing particles, a thinner target should be used.

The target thickness as well as the initial beam energy must be adapted in order to investigate a specific energy range in the excitation energy of the compound nucleus.

The upper edge and the lower edge in the elastic recoil spectrum correspond respectively to the initial beam energy (highest E_{CM}) and to the final beam energy (lowest E_{CM}) after the slowing down in the target (see fig. 1, light grey shadowed zone). The experimental limitation of the TTIK method is represented by the contamination, coming from other possible reaction mechanisms (like inelastic scattering), of the final elastic scattering excitation function.

This means that recoil particles reaching the detectors at the same energy can be generated by different reaction mechanisms (see fig. 2). This implies different paths inside the target for different classes of events. It is possible to experimentally disentangle the elastic cross-section excitation function from the inelastic contribution by choosing an

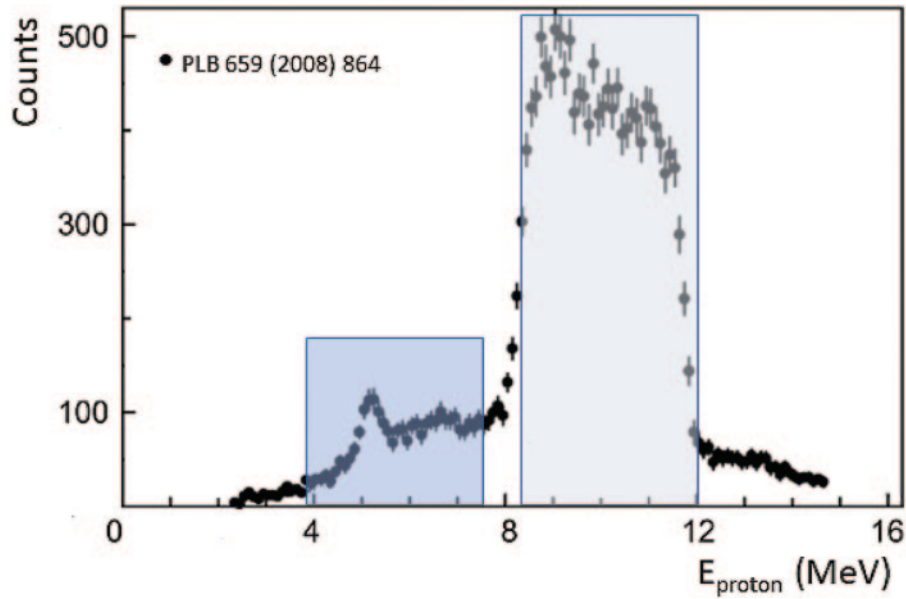


Fig. 1. – Data from [4]. Due to the choice of the target thickness, elastic events (light grey shadowed region) are disentangled from inelastic events (light blue shadowed region).

appropriate target thickness. In fig. 1, data from $^{18}\text{Ne} + p$ elastic scattering measured from [4] are reported. The elastic excitation function, light grey shadowed zone, is energetically disentangled from the inelastic contribution, $^{18}\text{Ne}^* + p'$, light blue shadowed zone. If the target thickness is increased, the lower edge of the elastic scattering region (fig. 1, light grey shadowed zone) will overlap the inelastic region (fig. 1, light blue shadowed zone).

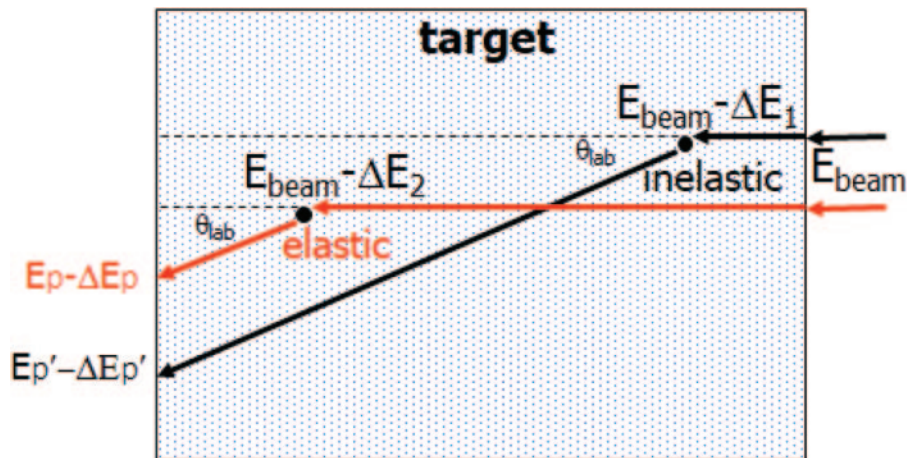


Fig. 2. – Pictorial view of two scattering events (inelastic in black and elastic in red), induced at two different E_{CM} energies (same initial beam energy). Due to energy loss effects, both ejectiles exit from the target with the same energy.

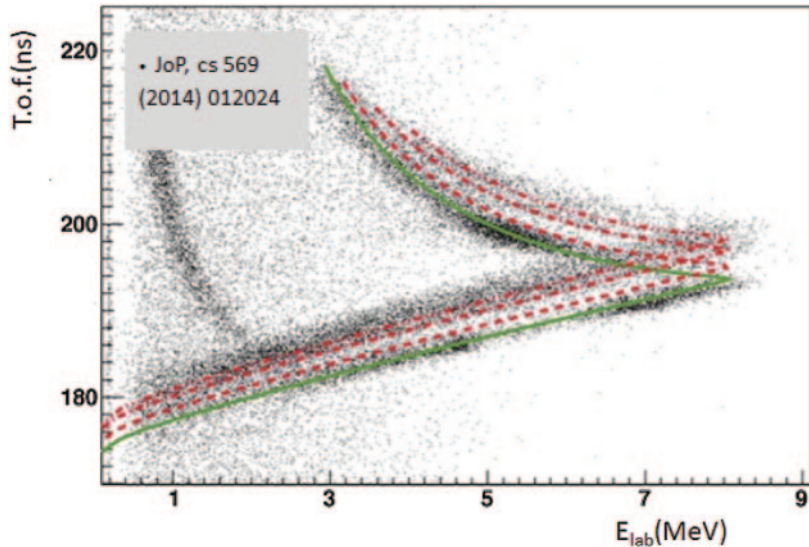


Fig. 3. – Data and calculation from [6]. ToF *vs.* detected ejectiles energy. Elastic scattering calculation is in green, inelastic scattering calculations are plotted in dashed red curves at three different excitation energies for ${}^8\text{Li}$.

4. – Gaseous targets and time-of-flight

The application of the TTIK method has some peculiarity for gaseous targets cases. Solid targets can be considered as point-like, being beam particles usually stopped in few millimeters. In gaseous targets, beam particles may have a long range (up to 1–2 m), depending on initial energy and gas pressure, with a ToF up to tens of ns. In this case, a ToF measurement can be performed to disentangle elastic scattering from other reaction contaminants, like inelastic scattering [5, 6].

This technique was based on the use of a wide scattering chamber filled with gas. The ToF was given by the sum of the time occurring to the beam to induce the interaction inside the target plus the time needed by the light ejectiles to reach the detector (usually placed at the most forward angles). It was measured by using the time signal (start) coming from the alpha particles hitting the detector and the signal (delayed stop) coming from a Micro Channel Plate (MCP) detecting the beam particles before entering in the gas chamber. This approach was used by [5] to study the ${}^9\text{Be}+{}^4\text{He}$ with results in agreement with direct kinematics measurements performed by [7–10]. The same technique was used by [6] to study the ${}^8\text{Li}+\alpha$ scattering. A ${}^8\text{Li}$ beam produced by the EXCYT facility at LNS-INFN Catania was sent to the LNS CT2000 chamber filled with ${}^4\text{He}$ gas. In this measurement it was possible to disentangle the elastic contribution from the inelastic one by plotting the ToF *vs.* the ejectiles energy (see fig. 3). A crucial parameter is the time resolution (~ 1 ns in [6]).

5. – A heavy ion case: ${}^{208}\text{Pb}+\alpha$ around the Coulomb barrier

A renewed interest has been recently devoted to the study of cluster structures in heavy ions [11]. In particular, the case of ${}^{212}\text{Po}$ was studied [12–15]. Astier *et al.* [12]

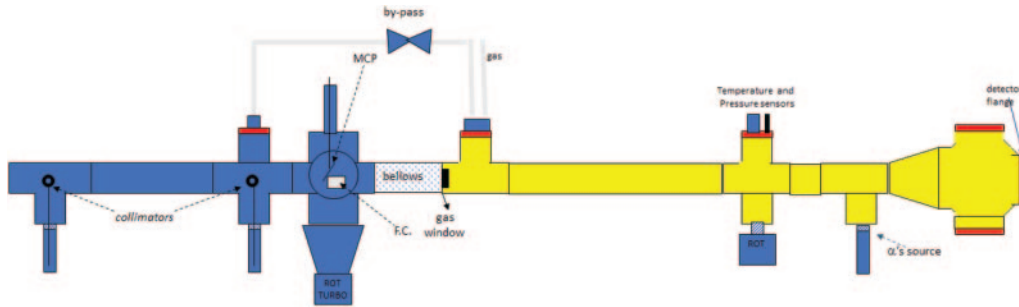


Fig. 4. – Experimental set-up used for the measurement of the $^{208}\text{Pb}+\alpha$ scattering at LNS-INFN. The gas chamber is filled with ^4He gas (yellow zone).

claim the discovery of low excited negative parity states in ^{212}Po in the E_x region below 3 MeV. They found very enhanced $E1$ transitions, which can be considered a signature of the α - ^{212}Pb oscillatory motion. According to Suzuki *et al.* [13] this experimental evidence has to be attributed to the strong contribution of an α - ^{208}Pb (3^- , 2.615 MeV) cluster state.

In order to further investigate the α - ^{208}Pb structure in ^{212}Po , the elastic scattering $^4\text{He}(^{208}\text{Pb}, \alpha)^{208}\text{Pb}$ was studied around the Coulomb barrier by using the TTIK method at INFN-Laboratori Nazionali del Sud, Catania.

A 31^+ charge state ^{208}Pb beam, extracted from the SERSE ECR source at Laboratori Nazionali del Sud, was accelerated at 10.1 AMeV by the Superconducting Cyclotron. The beam was first collimated (see fig. 4) and before reaching the gas target (yel-

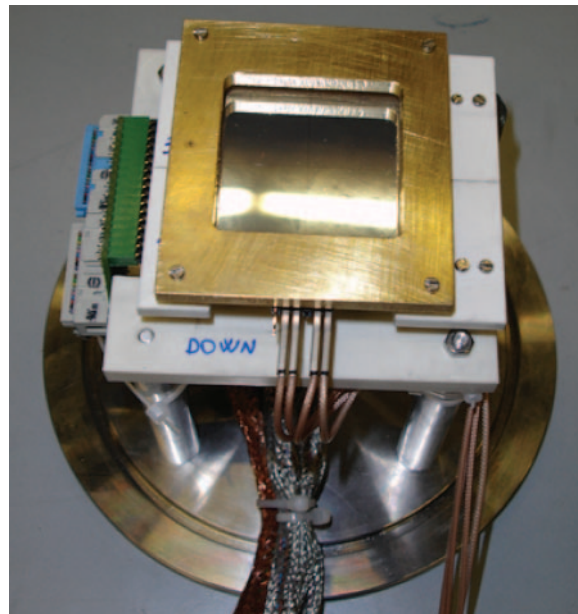


Fig. 5. – Picture of the first detector set-up. A collimator is placed in front of a three-stages silicon telescope.

low zone in fig. 4) was detected by using a MCP. The MCP signal provided a reference for ToF measurement and, at the same time, allows beam particle counting. The beam was impinging on the ^4He gas target, coupled with the beam line by an Al window. Gas pressure and temperature were measured by using an absolute pressure gauge (MKS Baratron 122 A) and a Pt100 probe, respectively. During the experiment two different detector set-ups were used. The first set-up (see fig. 5) was a three-stages detector: a four quadrant Si detector ($60\ \mu\text{m}$ thick) and two Double Sided Silicon Strip Detectors (DSSSDs), as second and third stage ($492\ \mu\text{m}$ and $1003\ \mu\text{m}$ thick, respectively). A collimator and a catcher ($25\ \mu\text{m}$ thick) were placed in front of the detector system. The second set-up was based on an ORTEC silicon surface-barrier detector, with a thickness of $1031\ \mu\text{m}$. Both detectors systems were alternatively placed at the most forward angles.

In the following, we will refer to the preliminary results obtained by the first set-up placed at zero degree detecting the recoiling alpha particles. Preliminary results of the second set-up are described in [16].

In this detector configuration, the second stage DSSSD ($492\ \mu\text{m}$ thick) was used as start detector (trigger) for ToF measurement. The stop signal was provided by the MCP detecting the primary ^{208}Pb beam particles. The overall ToF time resolution was measured to be $\sim 1\ \text{ns}$. Stopping power measurements of ^{208}Pb in ^4He have also been performed. As stated by Zadro *et al.* [5], this is essential in order to recover the beam energy for a given scattering event.

The detector energy calibration was performed by using an ^{241}Am - ^{244}Cu - ^{239}Pu alpha source, a ^4He beam at $10.1104\ \text{MeV/u}$ and the ADC pedestal. The ToF was calibrated by using different delays, namely: 8, 16 and 24 ns. ToF *vs.* detected energy 2D-spectrum is plotted in fig. 6. In a preliminary analysis, with low statistics, elastic scattered alpha particles appear as the main contribution. The analysis was performed by selecting the four central pixels of the second stage DSSSD, E_{CM} was recovered from alphas detected

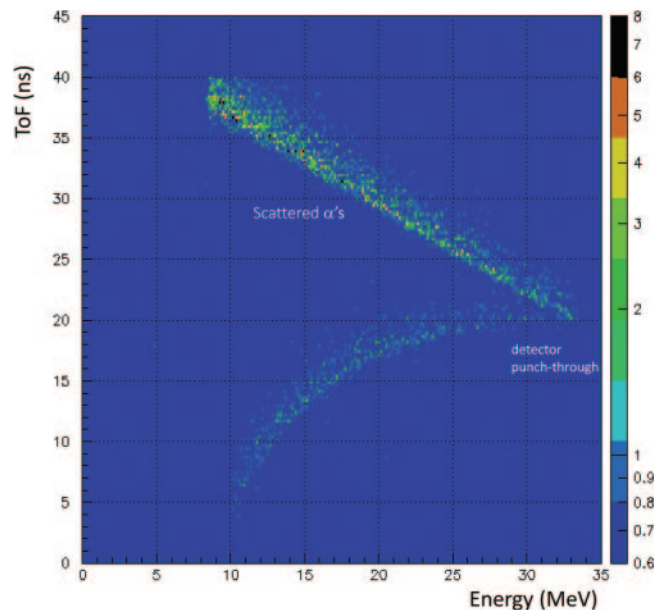


Fig. 6. – ToF *vs.* detected ejectiles energy for the ^{208}Pb - α elastic scattering (present data).

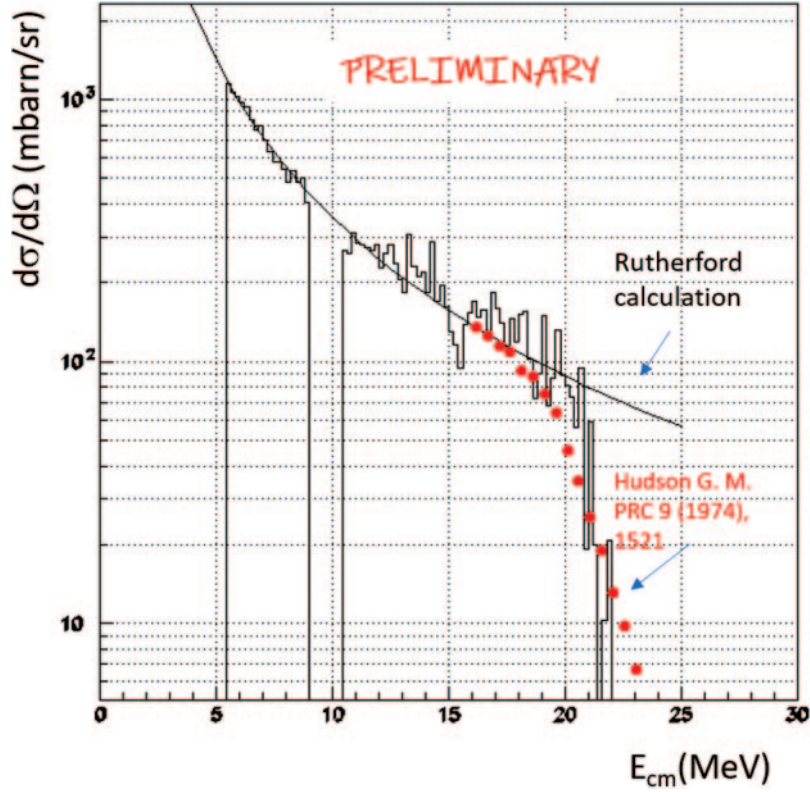


Fig. 7. – TTIK differential cross-section for the $^{208}\text{Pb}-\alpha$ elastic scattering (histogram). Rutherford calculation for the $^{208}\text{Pb}-^4\text{He}$ system (black line). $^4\text{He}+^{208}\text{Pb}$ direct kinematics measurement (red dots) [17].

energy by using LISE++ tools. A correction for the detector solid angle was applied in order to obtain the elastic cross-section. Finally, the experimental cross-section was normalised to the Rutherford cross-section to obtain the absolute cross-section shown in fig. 7.

As shown in fig. 7, the experimental trend (histogram) agrees with the Rutherford cross-section at low energy (black line). Around the Coulomb barrier, which is 26 MeV for the α - ^{208}Pb system, the trend is in agreement with the experimental cross-section measured in direct kinematics by [17] (red points in fig. 7). The particle punching-through in the second stage detector corresponds to E_{CM} between 9 and 10.5 MeV. The statistical error bar is $\sim 3\%$ at 5.5 MeV. A GEANT-4 simulation is in progress in order to take into account the set-up geometry and energy losses.

6. – Conclusions

The TTIK method is a powerful tool to investigate resonances in a compound nucleus by using a single mono-energetic heavy-ion beam. The use of the ToF technique allows the discrimination of elastic scattering from other reaction mechanism (like inelastic scattering) [5, 6].

Preliminary results on $^{208}\text{Pb}+^4\text{He}$ around the Coulomb barrier show that the TTIK method is suited also to be used with high projectile atomic mass number (^{208}Pb case).

The experimental cross-section trend is in agreement with a Rutherford calculation at low energy and with the direct kinematics measurement at high energy. Further data analysis, using the full data set, is in progress in order to study the contaminants of the elastic scattering contribution, in the ToF *vs.* energy spectrum, and to investigate the presence of deviation from Coulomb behaviour, which are signatures of states in ^{212}Po compound nucleus.

* * *

The authors acknowledge LNS-INFN staff for the support in the preparation of the POLONIUM experiment and the tuning of the ^{208}Pb beam.

REFERENCES

- [1] ARTEMOV K. P., BELYANIN P. and VETOSHKIN A. L., *Sov. J. Nucl. Phys.*, **52** (1990) 408.
- [2] GOLDBERG V. Z., ROGACHEV G. V., TRZASKA W. H., KOLATA J. J., ANDREYEV A., ANGULO C., BORGE M. J. G., CHERUBINI S., CHUBARIAN G., CROWLEY G., VAN DUPPEN P., GORSKA M., GULINO M., HUYSE M., JESINGER P., KLLMAN K.-M., LATTUADA M., LNNROTH T., MUTTERER M., RAABE R., ROMANO S., ROZHKOVA M. V., SKORODUMOV B. B., SPITALERI C., TENGBLAD O. and TUMINO A., *Phys. Rev. C*, **69** (2004) 024602.
- [3] ANGULO C., TABACARU G., COUDER M., GAELENS M., LELEUX P., NINANE A., VANDERBIST F., DAVINSON T., WOODS P. J., SCHWEITZER J. S., ACHOURI N. L., ANGLIQUE J. C., BERTHOUMIEUX E., DE OLIVEIRA SANTOS F., HIMPE P. and DESCOUVEMONT P., *Phys. Rev. C*, **67** (2003) 014308.
- [4] PELLEGRITI M. G., ACHOURI N. L., ANGULO C., ANGLIQUE J.-C., BERTHOUMIEUX E., CASAREJOS E., COUDER M., DAVINSON T., GHAG C., MURPHY A., ST. ORR N. A., RAYE I., STEFAN I. G. and DESCOUVEMONT P., *Phys. Lett. B*, **659** (2003) 864.
- [5] ZADRO M., DI PIETRO A., FIGUERA P., FISICHELLA M., LATTUADA M., MAGGIO A., PANSINI F., PAPA M., SCUDERI V., GORYUNOV O. YU. and OSTASHKO V. V., *Nucl. Instrum. Methods B*, **259** (2007) 836.
- [6] TORRESI D., COSENTINO L., DESCOUVEMONT P., DI PIETRO A., DUCOIN C., FIGUERA P., FISICHELLA M., LATTUADA M., MAIOLINO C., MUSUMARRA A., PAPA M., PELLEGRITI M. G., ROVITUSO M., SANTONOCITO D., SCALIA G., SCUDERI V., STRANO E. and ZADRO M., *J. Phys. Conf. Ser.*, **569** (2014) 012024.
- [7] GOSS J. D., BLATT S. L., PARSONS D. R., PORTERFIELD C. D. and RIFLE F. L., *Phys. Rev. C*, **7** (1973) 1837.
- [8] LIU J., ZHENG Z. and CHU W. K., *Nucl. Instrum. Methods B*, **108** (1996) 247.
- [9] LOMBARDO I., CAMPAJOLA L., DELL'AQUILA D., LA COMMARA M., ORDINE A., ROSATO E., SPADACCINI G. and VIGILANTE M., *J. Phys. Conf. Ser.*, **569** (2014) 012068.
- [10] LOMBARDO I., DELL'AQUILA D., SPADACCINI G., VERDE G. and VIGILANTE M., *Phys. Rev. C*, **97** (2018) 034320.
- [11] REN ZHONGZHOU and ZHOU BO, *Front. Phys.*, **13** (2018) 132110.
- [12] ASTIER A., PETKOV P., PORQUET M.-G., DELION D. S. and SCHUCK P., *Phys. Rev. Lett.*, **104** (2010) 0427701.
- [13] SUZUKI Y. and OHKUBO S., *Phys. Rev. C*, **82** (2010) 041303(R).
- [14] IBRAHIM T. T., PEREZ S. M. and WYNGAARDT S. M., *Phys. Rev. C*, **82** (2010) 034302.
- [15] NI DONGDONG and REN ZHONGZHOU, *Phys. Rev. C*, **83** (2011) 014310.
- [16] PELLEGRITI M. G., MUSUMARRA A., DE FILIPPO E., DE NAPOLI M., DI PIETRO A., FIGUERA P., FISICHELLA M., MAIOLINO C., RIFUGGIATO D., SANTONOCITO D., SCUDERI V., STRANO E. and TORRESI D., *EPJ Web of Conferences*, **223** (2019) 01049.
- [17] HUDSON G. M. and DAVIS R. H., *Phys. Rev. C*, **9** (1974) 152.